

Cold CO gas in the disk of the young eruptive star EX Lup

Á. Kóspál^{1,2}, P. Ábrahám¹, T. Csengeri³, U. Gorti^{4,5}, Th. Henning², A. Moór¹, D. A. Semenov², L. Szűcs⁶, R. Güsten³

Received _____; accepted _____

To appear in ApJL

¹Konkoly Observatory, Research Centre for Astronomy and Earth Sciences, Hungarian Academy of Sciences, P.O. Box 67, 1525 Budapest, Hungary

²Max-Planck-Institut für Astronomie, Königstuhl 17, 69117 Heidelberg, Germany

³Max-Planck-Institut für Radioastronomie, Auf dem Hügel 69, 53121 Bonn, Germany

⁴SETI Institute, Mountain View, CA

⁵NASA Ames Research Center, Moffett Field, CA

⁶Max-Planck-Institut für Extraterrestrische Physik, 85741 Garching, Germany

ABSTRACT

EX Lupi-type objects (EXors) form a sub-class of T Tauri stars, defined by sudden sporadic flare-ups of 1-5 magnitudes at optical wavelengths. These eruptions are attributed to enhanced mass accretion from the circumstellar disk to the star, and may constitute important events in shaping the structure of the inner disk and the forming planetary system. Although disk properties must play a fundamental role in driving the outbursts, they are surprisingly poorly known. In order to characterize the dust and gas components of EXor disks, here we report on observations of the ^{12}CO J=3–2 and 4–3 lines, and the ^{13}CO 3–2 line in EX Lup, the prototype of the EXor class. We reproduce the observed line fluxes and profiles with a line radiative transfer model, and compare the obtained parameters with corresponding ones of other T Tauri disks.

Subject headings: stars: pre-main sequence — stars: variables: T Tauri — stars: individual(EX Lup)

1. Introduction

EX Lup is the prototype of EXors, one of the two main classes of young eruptive stars. EXors are young low-mass T Tauri stars exhibiting repetitive outbursts due to a sudden increase of the accretion rate (Herbig 1977, 2008). In 2008, EX Lup exhibited its largest outburst ever observed, triggering a series of multi-wavelength and multi-epoch investigations of the accretion process. These led to the discovery of the annealing of amorphous silicate particles to crystalline grains during the outburst and their transportation to the outer comet-forming zone (Ábrahám et al. 2009; Juhász et al. 2012). Changes in the molecular features of H_2O , OH, and H_2 indicate that the outburst affected not only the surface mineralogy, but also the chemistry in the inner disk (Banzatti et al. 2012). Using high resolution spectroscopic and spectroastrometric tools, Goto et al. (2011), Kóspál et al. (2011), and Sicilia-Aguilar et al. (2012) concluded that the high accretion rate responsible for the outburst mostly affected the innermost 0.4 au region. They detected an accretion-related wind and the motion of non-axisymmetric distribution of material in the inner disk.

The emerging picture is broadly consistent with the magnetospheric accretion scenario, in which the infalling material reaches the star in hot spots. Indeed, X-ray and UV observations by Grosso et al. (2010) and by Teets et al. (2012) indicate accretion shocks. Recently, Kóspál et al. (2014) and Sicilia-Aguilar et al. (2015) studied the radial velocity variations of optical absorption and emission lines, and discussed different interpretation in terms of a possible brown dwarf companion on a tight eccentric orbit around EX Lup, or emission from stable accretion columns in the system.

All the observations summarized above concentrated on the inner part of the disk, within a few au of the star. However, the structure and dynamics of the outer disk must play a significant role in driving the outburst by replenishing the material in the inner

disk after each eruption. It is an open question whether the outer disks of EXors differ in any way from the disks of normal T Tauri stars. A negative answer could suggest that all low-mass stars undergo EXor phases during their early evolution.

Very few information is available on the outer disk or on global disk properties of the prototype, EX Lup. The emission of the cold dust component was detected at infrared wavelengths (Gras-Velázquez & Ray 2005; Sipos et al. 2009), and at $870\,\mu\text{m}$ with APEX/LABOCA (Juhász et al. 2012). Modeling the spectral energy distribution (SED) based on these data, Sipos et al. 2009 and Juhász et al. (2012) deduced a modestly flared disk geometry. In the lack of spatially resolved infrared or millimeter data, the outer disk radius of EX Lup is unknown. Much less is known about the gas component. Warm carbon monoxide (CO) gas was detected in the fundamental lines at $4.5\,\mu\text{m}$ and in the overtone band at $2.3\,\mu\text{m}$ (Aspin et al. 2010; Goto et al. 2011; Kóspál et al. 2011). The profiles of the fundamental lines could be well fitted with an inner disk inclination angle between 40° and 50° (Goto et al. 2011). Concerning the cold gas in the disk, the only available millimeter CO observation reported in the literature, a $^{12}\text{CO}(3-2)$ line targeted by van Kempen et al. (2007) using JCMT, was a non-detection.

In order to study the abundance, distribution, and kinematics of cold molecular gas in EX Lup’s disk, we obtained new submillimeter CO line observations with APEX/FLASH⁺. In this Letter, we present the data and analyze the line profiles, line intensities, measure the CO mass, optical depth, reproduce the results with a chemical and radiative transfer model, and confront the results with those obtained for typical T Tauri-type stars.

2. Observations

We used the FLASH⁺ receiver (Klein et al. 2012) at the APEX telescope (Güsten et al. 2006) to measure the $^{12}\text{CO}(3-2)$, $^{13}\text{CO}(3-2)$, and $^{12}\text{CO}(4-3)$ lines towards EX Lup on 2015 March 30 – April 1. The lower frequency channel was tuned to 344.2 GHz in USB to cover the $^{13}\text{CO}(3-2)$ at 330.588 GHz, and the $\text{CO}(3-2)$ at 345.796 GHz, respectively. The higher frequency channel was tuned to the $^{12}\text{CO}(4-3)$ line at 461.041 GHz in USB. We used the XFFTS backends providing a nominal 38.15 kHz spectral resolution. Observations were carried out in position switching mode with a relative reference position 100'' away.

The spectra have been averaged and a first order baseline has been removed. The noise level on a T_A^* scale in 1 km/s channels is 5.2 mK (0.21 Jy) for $^{12}\text{CO}(3-2)$, 11.5 mK (0.55 Jy) for $^{12}\text{CO}(4-3)$, and 7.7 mK (0.32 Jy) for $^{13}\text{CO}(3-2)$. We used a Jy-to-K conversion of 41 Jy/K for the 3–2 lines and 48 Jy/K for the 4–3 line to convert from T_A^* scale to flux scale. The telescope’s beam is 19''.2, and 15''.3 at the corresponding frequencies.

3. Results and Analysis

Our CO spectra are plotted in Fig. 1. The ^{12}CO lines are securely detected at 12σ and 7.7σ levels for the 3–2 and 4–3 lines, respectively. There is a marginal detection of the $^{13}\text{CO}(3-2)$ line at a level of 2.6σ , at the same radial velocity as the other CO lines. The observed lines are single-peaked. The peak fluxes, total line intensities, line widths (FWHM of fitted Gaussians), and line positions (centers of the fitted Gaussians) are presented in Tab. 1.

The ratio of the 3–2 lines of the two different CO isotopologues can be used to calculate the optical depths of the lines. If we denote the optical depths of ^{12}CO and ^{13}CO by τ_{12} and τ_{13} , respectively, then the ratio of the ^{12}CO to the ^{13}CO line is approximately

$(1 - e^{-\tau_{12}})/(1 - e^{-\tau_{13}})$. Assuming that the optical depths of the different isotopologues follow the same proportions as the abundance ratios typical of local interstellar matter (Wilson 1999), $\tau_{12} = 69 \times \tau_{13}$. Using these numbers, we obtained $\tau_{12} \approx 20$ and $\tau_{13} \approx 0.3$. Even considering the uncertainties in this evaluation, it is very likely that the ^{12}CO lines are optically thick, while the ^{13}CO line is optically thin.

The temperature of the CO gas can be estimated from the ratio of the optically thick $^{12}\text{CO}(4-3)$ and $^{12}\text{CO}(3-2)$ lines. In the Rayleigh–Jeans approximation, the ratio is expected to be the ratio of the squares of the line frequencies, i.e., about 1.78. Instead, using the total flux values from Tab. 1, we obtain 1.25 ± 0.15 , significantly different from the Rayleigh–Jeans value. The low value suggests that the temperature is very low and that the Rayleigh–Jeans approximation is not valid. Indeed, using the Planck function, this line ratio corresponds to 10_{-2}^{+4} K.

From the optically thin ^{13}CO line, using the canonical 10^{-4} CO-to- H_2 abundance ratio, we estimate a total disk mass of $2.3 \times 10^{-4} M_{\odot}$. If the abundance ratio is lower than 10^{-4} , as will be discussed in Sect. 5.2, then this disk mass should be considered as a lower limit.

4. Chemical and Radiative Transfer Modeling

In order to reproduce the observed line profiles and line fluxes, we made a detailed chemical and radiative transfer model of the EX Lup disk. As a base, we used the model of Sipos et al. (2009) to fit the quiescent spectral energy distribution (SED), providing radial and vertical dust density and dust temperature distributions. We used this physical model and performed a detailed simulation of the disk chemistry similarly to that described in Gorti et al. (2011). The CO abundance, densities, and temperatures were calculated without assuming local thermodynamical equilibrium (LTE), and included radiative

pumping, dust background radiation, and spontaneous emission and collisions. In parallel, we verified the results with the state-of-the-art chemical code `ALCHEMIC` (Semenov et al. 2010), and found similar results. The obtained gas-phase ^{12}CO fractional abundances were used as input for our line transport calculations, performed with the `RADMC-3D` code¹. We assumed a homogeneous gas-to-dust ratio of 100 and a Keplerian velocity field with a microturbulent velocity of 0.1 km/s, taken to be constant throughout the disk. The abundances of ^{13}CO and C^{18}O were calculated using a constant $^{12}\text{CO}/^{13}\text{CO}$ ratio of 69 and $^{12}\text{CO}/\text{C}^{18}\text{O}$ ratio of 560 (Wilson 1999). The obtained densities and temperatures imply that LTE holds everywhere in the disk, thus we adopted LTE for modeling the line profiles. The gas temperature was assumed to be equal with the dust temperature. The line emission was calculated in 8 km/s wide windows centered on the rest frame wavelengths of the J=3–2 and 4–3 transitions of ^{12}CO and ^{13}CO .

In Fig. 1 we overplotted the resulting model spectra. In order to match the brightness of the observed lines, the gas temperature in our model had to be scaled down by a factor of 0.8. With this small modification, all measured line fluxes and line ratios are well reproduced by our model, indicating that the disk parameters responsible for the line width were reasonable estimates. This result also confirms that the inclination of 40° used in the radiative transfer calculations is good approximation. The double-peaked profiles characteristic for a disk in Keplerian orbit are not observed probably due to the limited spectral resolution of the data. We emphasize that while our modeling provides a possible solution to reproduce the observed lines, it was not a fit to the lines. The exploration of the full parameter space needed to prove that this is a unique solution is beyond the scope of this Letter. For this reason, in the following, we base our discussion on our measured CO line fluxes.

¹<http://www.ita.uni-heidelberg.de/~dullemond/software/radmc-3d/>

5. Discussion

5.1. Disk mass from dust continuum data

Sipos et al. (2009) assumed small grains and fitted the SED with a total disk mass of $0.025 M_{\odot}$. Sicilia-Aguilar et al. (2015) could obtain a reasonably well fit to the SED with a total mass of $1\text{--}3 \times 10^{-3} M_{\odot}$ by using grains between 0.1 and $100 \mu\text{m}$ with collisional size distribution. In these studies, when converting the dust mass to total mass, a gas-to-dust mass ratio of 100 was assumed. While this is typical for the interstellar medium (ISM), circumstellar disks often have lower gas-to-dust mass ratios. Recently, Williams & Best (2014) measured values between 43 and 2 for T Tauri stars in Taurus, based on Submillimeter Array (SMA) observations of the 1.3 mm continuum and $^{13}\text{CO}(2\text{--}1)$ and $\text{C}^{18}\text{O}(2\text{--}1)$ lines. Considering these uncertainties, the total disk mass of EX Lup from dust continuum data may be as high as $0.025 M_{\odot}$ (using small grains and gas-to-dust ratio of 100) or as low as a few times $10^{-4} M_{\odot}$ (using a grain size distribution and a gas-to-dust ratio of 10). While the lower value is roughly consistent with the disk mass obtained from our ^{13}CO data, the higher value is about 100 times higher, hinting at significant CO depletion in the disk of EX Lup.

5.2. CO depletion in EX Lup

In order to find out whether the disk properties derived from our CO observations of EX Lup are in any way special, we need to compare it to normal, non-eruptive young stars. Thi et al. (2001) observed the $^{13}\text{CO}(3\text{--}2)$ line in eight T Tauri-type stars and in seven Herbig Ae stars in the Taurus-Auriga cloud, calculated the total gas masses, and compared them with total masses inferred from 1.3 mm dust continuum measurements. They found that “masses derived from CO are generally 10-200 times lower than those

found from the millimeter continuum”. In Fig. 2 we reproduced Fig. 10 from Thi et al. (2001), and overplotted EX Lup, using the same equations and assumptions to calculate the disk masses as was used in that paper (we estimated a range of 1.3 mm fluxes for EX Lup by extrapolating from the 870 μ m flux presented in Juhász et al. 2012 using $\beta=0\ldots1.7$ as the spectral index of the dust opacity). Compared to the sample of Thi et al. (2001), EX Lup has a remarkably small disk mass and modest CO depletion. This result means that the total disk mass might be a factor of 10...100 higher than the value calculated in Sect. 3.

Thi et al. (2001) listed two possible reasons for the CO depletion: (1) freeze-out in the coldest, mid-plane regions of the disk (indeed, Reboussin et al. (2015) found that the canonical gas-phase abundance of CO compared to H₂ of 10^{-4} is only reached above about 30 – 35 K, below this temperature, the ratio is much smaller because CO depletion due to freeze-out is very efficient); (2) photodissociation by stellar or interstellar UV radiation in the disk surface. These two effects may operate in EX Lup as well. Firstly, according to our radiative transfer model, the dust temperature in the disk midplane in the outer disk regions is indeed below 15 K, therefore CO is expected to freeze out. Secondly, the two M-type stars in the sample of Thi et al. (2001) show similar CO depletion factor (about 100), indicating similar radiation fields.

The fact that the CO depletion in EX Lup is less than those observed in normal T Tauri and most of those in Herbig Ae stars as well has interesting implications. EX Lup exhibited a large outburst in 2008, when both its optical and X-ray brightness increased by orders of magnitude (Kóspál et al. 2008; Teets et al. 2012). According to our modeling, both the midplane and the surface temperature increased in the disk during outburst (Ábrahám et al. 2009). On the one hand, the increased temperature might have evaporated CO ice and increased the abundance of gas-phase CO, as predicted by Vorobyov et al. (2013). On the other hand, the increased UV flux during outburst might have photodissociated a

significant amount of CO gas. It seems that in the case of EX Lup, the latter effect was more dominant. Our low-J CO observations trace the bulk of the cold gas, therefore the outburst affected the outer parts of the disk, and not only its innermost part (where Banzatti et al. 2015 found a depletion of hot CO after the outburst, interpreted as depletion of material accumulated around and within the corotation radius at 0.02–0.3 au). Our observations support the conclusions of Vorobyov et al. (2013), whose numerical simulations showed that the chemical signatures of luminosity bursts in the gas-phase CO abundance may linger for several thousand years.

5.3. The mechanism of EXor outbursts?

Liu et al. (2016) observed four EXors in the 1.3 mm continuum with the SMA. They detected two targets, one with a relatively high dust mass (NY Ori, $9 \times 10^{-4} M_{\odot}$), and one with much lower (V1118 Ori, $6 \times 10^{-5} M_{\odot}$). The other two targets were undetected, with 3σ upper limits of $6 \times 10^{-5} M_{\odot}$ for V1143 Ori and $6 \times 10^{-6} M_{\odot}$ for VY Tau. Compared to these, the dust disk mass of EX Lup is in the range of the least massive EXor disks detected. Therefore, the prototype of the class fits into the trend that EXors disks are less massive than FUor disks. A possible cause for the low disk masses is binarity: there is a trend that stars with companions within 100 au generally have lower disk masses than single stars or wider binaries (Osterloh & Beckwith 1995; Andrews & Williams 2005). Indeed, many EXors are binaries (e.g., VY Tau, V1118 Ori, or XZ Tau, see Leinert et al. 1993, Reipurth et al. 2007, Hartigan & Kenyon 2003). EX Lup have been searched for companions with different methods without conclusive results (see, e.g., Kóspál et al. 2014 and references therein).

The low EXor disk masses raise the question what mechanism causes the eruption of these disks and what reservoir can replenish the material in the inner disk after it lands

on the star. The low disk masses virtually exclude mechanisms related to gravitational instability. A promising new idea was presented by D’Angelo & Spruit (2012), who proposed that accretion onto a strongly magnetic protostar is inherently episodic if the disk is truncated close to the corotation radius. D’Angelo & Spruit (2012) demonstrated that this mechanism may work for EX Lup.

This work was supported by the Momentum grant of the MTA CSFK Lendület Disk Research Group, and the Hungarian Research Fund OTKA grant K101393. A. M. acknowledges support from the Bolyai Research Fellowship of the Hungarian Academy of Sciences.

Facilities: APEX.

REFERENCES

- Ábrahám, P., Juhász, A., Dullemond, C. P., et al. 2009, *Nature*, 459, 224
- Andrews, S. M., & Williams, J. P. 2005, *ApJ*, 631, 1134
- Aspin, C., Reipurth, B., Herczeg, G. J., & Capak, P. 2010, *ApJ*, 719, L50
- Banzatti, A., Pontoppidan, K. M., Bruderer, S., Muzerolle, J., & Meyer, M. R. 2015, *ApJ*, 798, L16
- Banzatti, A., Meyer, M. R., Bruderer, S., et al. 2012, *ApJ*, 745, 90
- D’Angelo, C. R., & Spruit, H. C. 2012, *MNRAS*, 420, 416
- Gorti, U., Hollenbach, D., Najita, J., & Pascucci, I. 2011, *ApJ*, 735, 90
- Goto, M., Regály, Z., Dullemond, C. P., et al. 2011, *ApJ*, 728, 5
- Gras-Velázquez, À., & Ray, T. P. 2005, *A&A*, 443, 541
- Grosso, N., Hamaguchi, K., Kastner, J. H., Richmond, M. W., & Weintraub, D. A. 2010, *A&A*, 522, A56
- Güsten, R., Nyman, L. Å., Schilke, P., et al. 2006, *A&A*, 454, L13
- Hartigan, P., & Kenyon, S. J. 2003, *ApJ*, 583, 334
- Herbig, G. H. 1977, *ApJ*, 217, 693
- . 2008, *AJ*, 135, 637
- Juhász, A., Dullemond, C. P., van Boekel, R., et al. 2012, *ApJ*, 744, 118
- Klein, B., Hochgürtel, S., Krämer, I., et al. 2012, *A&A*, 542, L3

- Kóspál, A., Németh, P., Ábrahám, P., et al. 2008, *Information Bulletin on Variable Stars*, 5819, 1
- Kóspál, Á., Ábrahám, P., Goto, M., et al. 2011, *ApJ*, 736, 72
- Kóspál, Á., Mohler-Fischer, M., Sicilia-Aguilar, A., et al. 2014, *A&A*, 561, A61
- Leinert, C., Zinnecker, H., Weitzel, N., et al. 1993, *A&A*, 278, 129
- Liu, H. B., Galván-Madrid, R., Vorobyov, E. I., et al. 2016, *ApJ*, 816, L29
- Osterloh, M., & Beckwith, S. V. W. 1995, *ApJ*, 439, 288
- Reboussin, L., Wakelam, V., Guilloteau, S., Hersant, F., & Dutrey, A. 2015, *A&A*, 579, A82
- Reipurth, B., Guimarães, M. M., Connelley, M. S., & Bally, J. 2007, *AJ*, 134, 2272
- Semenov, D., Hersant, F., Wakelam, V., et al. 2010, *A&A*, 522, A42
- Sicilia-Aguilar, A., Fang, M., Roccatagliata, V., et al. 2015, *ArXiv e-prints*
- Sicilia-Aguilar, A., Kóspál, Á., Setiawan, J., et al. 2012, *A&A*, 544, A93
- Sipos, N., Ábrahám, P., Acosta-Pulido, J., et al. 2009, *A&A*, 507, 881
- Teets, W. K., Weintraub, D. A., Kastner, J. H., et al. 2012, *ApJ*, 760, 89
- Thi, W. F., van Dishoeck, E. F., Blake, G. A., et al. 2001, *ApJ*, 561, 1074
- van Kempen, T. A., van Dishoeck, E. F., Brinch, C., & Hogerheijde, M. R. 2007, *A&A*, 461, 983
- Vorobyov, E. I., Baraffe, I., Harries, T., & Chabrier, G. 2013, *A&A*, 557, A35
- Williams, J. P., & Best, W. M. J. 2014, *ApJ*, 788, 59

Wilson, T. L. 1999, Reports on Progress in Physics, 62, 143

This manuscript was prepared with the AAS L^AT_EX macros v5.2.

Table 1. CO Observations of EX Lup.

Line	Frequency (GHz)	Peak (Jy)	Flux (Jy km/s)	Width (km/s)	Position (km/s)
¹² CO(3–2)	345.796	2.63 ± 0.21	9.74 ± 0.41	3.6 ± 0.2	3.6 ± 0.2
¹² CO(4–3)	461.041	4.24 ± 0.55	12.15 ± 1.34	2.6 ± 0.3	3.9 ± 0.2
¹³ CO(3–2)	330.588	0.82 ± 0.32	2.09 ± 0.74	2.7 ± 1.1	5.1 ± 0.5

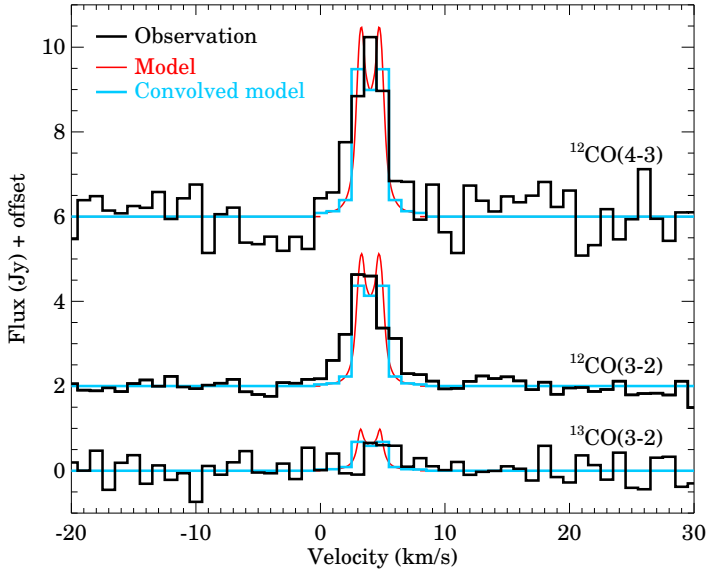


Fig. 1.— CO line profiles of EX Lup observed with APEX/FLASH⁺ (black histograms). The red curves are from our line radiative transfer model (for details, see Sec. 4). The blue histograms are the models convolved to the same spectral resolution as the observations.

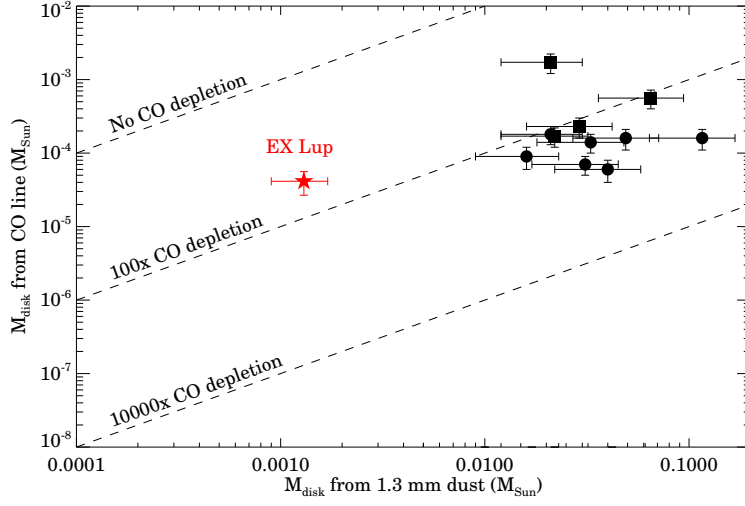


Fig. 2.— Disk masses estimated from CO observations against disk masses from dust continuum data (based on Fig. 10 of Thi et al. 2001). The black circles indicate T Tauri stars, the black squares mark Herbig Ae/Be stars, while EX Lup is plotted with a red asterisk.